

H₂ superglass on an amorphous carbon substrate

M. C. Gordillo*

*Departamento de Sistemas Físicos, Químicos y Naturales,
Universidad Pablo de Olavide, Carretera de Utrera km 1, E-41013 Sevilla, Spain and
Instituto Carlos I de Física Teórica y Computacional,
Universidad de Granada, E-18071 Granada, Spain*

J. Boronat

Departament de Física, Universitat Politècnica de Catalunya, Campus Nord B4-B5, 08034 Barcelona, Spain
(Dated: March 3, 2023)

The phase diagram of a *para*-H₂ monolayer adsorbed on an experimentally synthesized amorphous carbon sheet was calculated using a diffusion Monte Carlo technique. We found that the ground state of that system changed drastically from a perfectly flat substrate to a situation in which the carbon atoms were allowed a certain degree of disorder in the z direction. In the first case, at zero pressure we have a glass of density $0.056 \pm 0.003 \text{ \AA}^{-2}$ in equilibrium with an incommensurate solid of $0.068 \pm 0.002 \text{ \AA}^{-2}$. At the equilibrium density, the glass was found to have a tiny, but non-negligible superfluid fraction of less than 1 % (0.44 ± 0.05 %). In the z -disordered substrate, we observe a significant enhancement of the superfluid fraction in the glass phase as well as a smaller but not zero value in the incommensurate crystal.

It is well-known that the most stable form of carbon is graphite. It is also well-known that one can isolate one of those single carbon layers and obtain a stable structure termed graphene [1, 2]. Even though the electric properties of graphene are quite different from those of a three-dimensional arrangement [3, 4], theoretical calculations failed to find any significant difference between the adsorption behavior of quantum species (⁴He, H₂ and D₂) on graphene and graphite [5–7].

The honeycomb structure of graphene is made up exclusively of carbon hexagons, apart from occasional defects. However, amorphous structures, in which we can have carbon pentagons, hexagons and even squares in addition to six-fold rings, can be created by bombarding graphene with an electron beam [8, 9] or synthesized directly by chemical vapor deposition [10]. The main features of the latter structure can be captured by a two-dimensional $40 \times 40 \text{ \AA}^2$ patch (Supplementary information of Ref. 10) with no holes. The projection of those carbon coordinates in the $x-y$ plane are displayed in Fig. 1 as blue squares.

The goal of this work is to study the behavior of H₂ when adsorbed on an amorphous carbon surface. To do so, we will consider that substrate as adequately represented by the above coordinates, but bearing in mind that the carbon layer is not perfectly flat [10]. We solved the Schrödinger equation that describes the set of H₂ molecules on this new adsorbent using the diffusion Monte Carlo (DMC) method both in flat and corrugated carbon structures. Our results show that a stable H₂ glass phase is formed irrespectively of the substrate. That glass has a tiny superfluid fraction if the underlying carbon sheet is flat, fraction that is considerably enhanced for the z -disordered structure, i.e., we have an stable superglass. In the case of H₂, there is only a previous theoretical work that predicts a metastable three-dimensional superglass [11]. That glass would present a

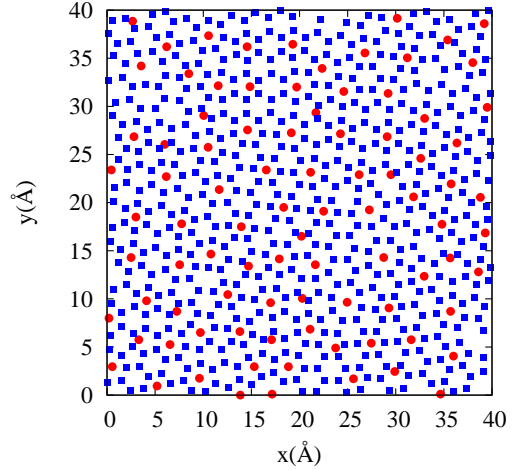


FIG. 1. Reconstruction of a monolayer amorphous carbon layer as given in Ref. 10. Blue squares, carbon atoms. Full red circles, adsorption positions for H₂ molecules at the equilibrium density of the glass for a planar surface.

sizeable superfluid density around ~ 1 K.

The DMC method allows for obtaining exactly the ground state of an ensemble of interacting bosons, within the statistical uncertainties inherent to any Monte Carlo technique [12]. To do so, we have first to write down the Hamiltonian describing a monolayer of hydrogen on top of the amorphous carbon substrate. This is:

$$H = \sum_{i=1}^N \left[-\frac{\hbar^2}{2m} \nabla_i^2 + V_{\text{ext}}(x_i, y_i, z_i) \right] + \sum_{i<j}^N V_{\text{H}_2-\text{H}_2}(r_{ij}) . \quad (1)$$

x_i , y_i , and z_i are the coordinates of the each of the N

H₂ molecules with mass m . $V_{\text{ext}}(x_i, y_i, z_i)$ is the interaction potential between each molecule and all the carbon atoms in the $40 \times 40 \text{ \AA}^2$ patch that models the amorphous structure. As in previous works [6, 13, 14], that interaction was chosen to be of the Lennard-Jones type, with parameters obtained from Ref. 15. $V_{\text{H}_2-\text{H}_2}$ is modeled by the standard Silvera and Goldman potential [16]. As indicated above, we consider two possibilities for the carbon substrate: a flat one, in which the carbon atoms are located in the $z = 0$ plane, and an irregular one, in which each z coordinate was chosen randomly in the interval $[-0.4, 0.4] \text{ \AA}$. This z -displacement is similar to the vertical distortion of the lattice found in previous ab initio calculations of amorphous graphite [17, 18]. To avoid the effects in the phase diagram of any particular z carbon distribution, all the simulations were repeated ten times with different carbon configurations and the results averaged over.

To actually solve the Schrödinger equation defined by the many-body Hamiltonian in Eq. 1, one uses a trial wave function to reduce the variance to a manageable level. We use a symmetrized Nosanow-Jastrow wave function split as the product of two terms, the first one being:

$$\Phi_J(\mathbf{r}_1, \dots, \mathbf{r}_N) = \prod_{i < j}^N \exp \left[-\frac{1}{2} \left(\frac{b}{r_{ij}} \right)^5 \right] \quad (2)$$

that depends on the distances, r_{ij} , between each pair of H₂ molecules and on b , a variationally optimized parameter whose value was found to be 3.195 \AA [6, 14]. The second one is:

$$\begin{aligned} \Phi_s(\mathbf{r}_1, \dots, \mathbf{r}_N) = & \prod_i^N \prod_J^{N_C} \exp \left[-\frac{1}{2} \left(\frac{b_C}{r_{iJ}} \right)^5 \right] \\ \times \prod_{I=1}^N \left[\sum_{i=1}^N \exp \{ -c [(x_i - x_{\text{site}, I})^2 + (y_i - y_{\text{site}, I})^2] \} \right] \\ & \times \prod_i^N \exp(-a(z_i - z_{\text{site}})^2) \quad (3) \end{aligned}$$

Here, b_C was chosen to be 2.3 \AA , as in previous works [6, 14]. The z_{site} and a values that minimize the energy in the infinite dilution limit were $z_{\text{site}} = 2.94 \text{ \AA}$ and $a = 3.06 \text{ \AA}^{-1}$. If we consider the H₂ phase to be translationally invariant $c = 0$, otherwise (i.e. for a solid or glass), $c = 0.61 \text{ \AA}^{-2}$. The latter value for c was taken from Ref. 6 in which it was variationally optimized for an incommensurate solid; nevertheless, we checked that changes in its value of up 50 % produced always worse energies when used in DMC. For both values of c the form of the *trial* function allows the H₂ molecules to be involved in exchanges and recover indistinguishability, something necessary if we are to consider the possibility of a stable superfluid. The same form of the trial function was used both for the flat and corrugated carbon substrates.

In Eq. 3, $(x_{\text{site}}, y_{\text{site}})$ are the positions of the nodes that define the network we are interested in. For an incommensurate hydrogen solid, those will be the coordinates of the crystallographic sites of the quasi-two dimensional triangular lattice. On the other hand, the glass is defined by a set of local energy minima irregularly arranged. To define those minima, we created a two-dimensional grid of regularly spaced points at a distance z_{site} above the carbon layer and calculated $V_{\text{ext}}(x, y, z_{\text{site}})$ at such positions. After that, we chose the point of the grid for which V_{ext} is minimum. Then, we searched for the point in the grid with the next-to-minimum value of the external potential located at a distance from the first of at least $\sigma_{C-\text{H}_2}$ (Lennard-Jones parameter of the C-H₂ interaction, 2.97 \AA [15]). This is done to avoid H₂-H₂ interactions that would contribute with positive terms to the total energy in the full DMC scheme. The entire process is iterated until it is not possible to locate more hydrogen molecules at distances of at least $\sigma_{C-\text{H}_2}$ from each other. After that, we are left with a list of $(x_{\text{site}}, y_{\text{site}})$ positions ordered from minimum to maximum *potential* energy. However, what we need is to have a list of nodes ordered from lowest to highest *total* energy. To get it, we performed DMC calculations including one single molecule on each of those sites and reordered the list with respect to those total single-molecule energies. By following that procedure we minimize the risk of getting metastable states once we start filling that network with H₂. This is so because the difference between the full DMC energy of a system of N molecules and the set of N increasing individual energies provided in the algorithm just described comes from the H₂-H₂ interaction. This contribution relies less and less on the details of the network for increasing density, since it depends primarily on the average first-neighbor distances. The number of maximum nodes found using this procedure was 104, and that was the maximum number of molecules used to describe the liquid and glass phases for the density range displayed in Fig. 2. On the other hand, that number oscillated between 90 and 120 for the incommensurate solid, the number of walkers in the DMC procedure being 300. The remaining of the simulation details are similar to those in Ref. 14 and omitted here for simplicity. The locations of the nodes of the glass are displayed in Fig. 1 as red circles on top of the carbon coordinates (blue squares). To be sure that the election of the cutoff distance does not change the nodes of the glass network, we repeated the entire procedure for exclusion values $\sigma_{C-\text{H}_2} \pm 10\%$, finding exactly the same positions for the minima. We checked also that for the densities considered in Fig. 2 to fill the glass network in a different order than the one described above, or to consider a different set of nodes (by starting the building up from another node), did not alter the total energies in the density range displayed there.

In Fig. 2, we show the energy per H₂ molecule as a function of the two-dimensional density for the three phases considered in this work: a liquid (full circles), an incommensurate triangular solid (full squares), and

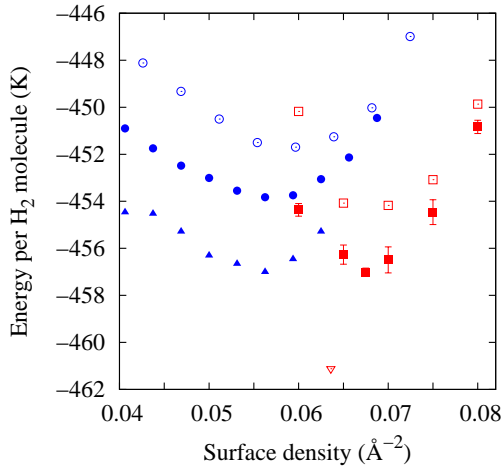


FIG. 2. Energy per H_2 molecule as a function of the density for hydrogen on top of flat graphene (open symbols) and amorphous carbon (full symbols). Circles, quasi two-dimensional liquid; squares, incommensurate triangular solid; full triangles, glass structure; open triangle, $\sqrt{3} \times \sqrt{3}$ structure on graphene. When not shown, error bars are of the size of the symbols.

a glass (full triangles) on a carbon flat amorphous substrate. In that figure, we display also the results for graphene, taken from Ref. [6]. Since both the graphene and the amorphous substrate have the same carbon density, 0.38 \AA^{-2} , this will allow us to assess the effects of the randomness on the phase diagram of the two-dimensional H_2 . What we see is that, at least in this case, the disorder in the substrate makes both the liquid and solid phases more stable than their corresponding counterparts in graphene. In any case, the triangular solid is still more stable than the liquid by 3.1 K at the densities corresponding to zero pressure (liquid binding energy, $453.8 \pm 0.5 \text{ K}$; solid binding energy $456.9 \pm 0.5 \text{ K}$). Obviously, the lack of periodicity makes impossible to have a commensurate structure, its place being taken by a glass arrangement of variable density. According to Fig. 2, the maximum binding energy for this structure is $457.0 \pm 0.5 \text{ K}$ at a density of $\rho = 0.056 \pm 0.003 \text{ \AA}^{-2}$. This density is appreciably smaller than the $0.068 \pm 0.002 \text{ \AA}^{-2}$ corresponding to the solid at the minimum of its curve, but equal to the one corresponding to the liquid structure ($\rho = 0.057 \pm 0.003 \text{ \AA}^{-2}$). However, the irregularity of the substrate produces a less stable phase than the $\sqrt{3} \times \sqrt{3}$ solid in graphene. In any case, from the results displayed in Fig. 2 we can draw an horizontal double-tangent Maxwell construction line between the minima of the glass and solid curves. This means that between 0.056 and 0.068 \AA^{-2} , we would have a mixture of a glass and a triangular solid in the adequate proportions to produce a system with the desired density. From $0.068 \pm 0.002 \text{ \AA}^{-2}$ up, the stable phase will be a triangular

solid.

A very recent calculation [14] suggests that we can find supersolid behavior for a H_2 second layer adsorbed on graphite in a very narrow density window around 0.1650 \AA^{-2} . By a supersolid we mean a solid structure (diagonal order) with a superfluid fraction different from zero (off-diagonal long-range order). By extension, a superglass would be a phase in which the molecules are arranged in an amorphous setup with a superfluid fraction larger than zero. Following the same procedure as in that work we estimated that fraction, ρ_s/ρ , both for the equilibrium densities of the glass and incommensurate triangular solids. To do so, we used, as in previous literature for similar systems [14, 19] the zero-temperature winding number estimator derived in Ref. 20,

$$\frac{\rho_s}{\rho} = \lim_{\tau \rightarrow \infty} \alpha \left(\frac{D_s(\tau)}{\tau} \right), \quad (4)$$

with τ the imaginary time used in the quantum Monte Carlo simulation. Here, $\alpha = N_2/(4D_0)$, $D_0 = \hbar^2/(2m)$, and $D_s(\tau) = \langle [\mathbf{R}_{CM}(\tau) - \mathbf{R}_{CM}(0)]^2 \rangle$. \mathbf{R}_{CM} is the position of the center of mass of the N H_2 molecules considering only their x and y coordinates. The results are shown in Fig. 3 for the glass phase. Each symbol correspond to an average of ten independent Monte Carlo histories for each value of imaginary time, the straight line being a least-squares fit to those points. The error bars correspond to the statistical noise. The superfluid fraction is the slope of the curve in the limit $\tau \rightarrow \infty$. In Fig. 3 we represent the that value instead of the equivalent average of $\alpha D_s(\tau)/\tau$ for each value of τ because in that way is easier to appreciate the superfluid fraction when its value is very small. The slope for the glass implies $\rho_s/\rho = 0.44 \pm 0.05 \%$, of the same order as the result in the second layer of graphite. To increase the number of Monte Carlo histories does not change the superfluid fraction within the error bar given for that magnitude. The corresponding curve for the incommensurate solid, not shown for simplicity, is completely flat, indicating a normal solid.

Since the amorphous carbon layer is not flat [10], we introduced some disorder in the z -direction to assess the effects of that randomness in the calculated observables. The results for the energies show again the same two stable structures. A double-tangent Maxwell construction indicates a first-order phase transition between a glass of density $0.055 \pm 0.003 \text{ \AA}^{-2}$, and a two-dimensional incommensurate crystal with $\rho = 0.0650 \pm 0.0025 \text{ \AA}^{-2}$. This means that the locus of the coexistence region is basically untouched by the introduction of disorder in z . However, the change in the superfluid character of the two phases is much relevant. The results obtained are shown in Fig. 4. This figure is similar to Fig. 3 but, instead of depicting the movement of the center of mass, it shows the full superfluid estimator as defined in Eq. 4. The values represented are $\rho_s/\rho = 0.21 \pm 0.05$ for a glass of density 0.053 \AA^{-2} (upper triangles), and $\rho_s/\rho = 0.14 \pm 0.05$ for a triangular solid with $\rho = 0.065 \text{ \AA}^{-2}$. Therefore, our

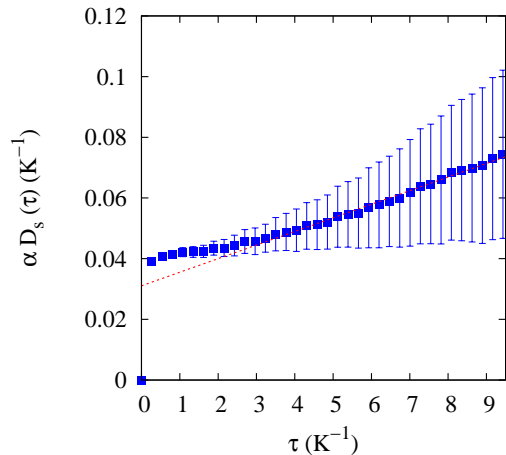


FIG. 3. Estimator of the superfluid density for the glass phase at its equilibrium density Full squares, simulation results. The straight line represent a linear least-squares fit to the symbols displayed for $\tau > 3 \text{ K}^{-1}$. Since the slope is different from zero, the disordered structure is a superglass.

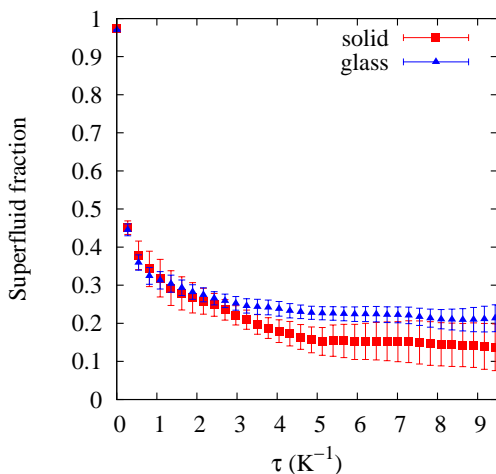


FIG. 4. Superfluid fraction for the irregular substrate. for two different phases and densities. Full triangles, glass phase of density $\rho = 0.053 \text{ \AA}^{-2}$; full squares, triangular solid with $\rho = 0.065 \text{ \AA}^{-2}$.

results show that we should have a superglass around a density around 0.055 \AA^{-2} , independently of the disorder of the substrate in the z direction. Moreover, the disorder in z induces supersolidity also in the incommensurate solid phase, in contrast with the flat adsorption surface.

The finite value of the superfluid fraction in both phases means that particles do not remain isolated around the lattice points but interchanges are possible. To show how this feature is observed in the DMC simulations, we plot in Fig. 5 some snapshots for both the glass and incommensurate crystal for the z -disordered carbon

substrate. Different colors stand for different set of walkers (particle configurations) corresponding to different Monte Carlo steps along the simulation. The spreading of every cloud is an indication of the quantum delocalization of the particles. One can see that these clouds are mainly located around the nodes of the respective lattices (glass or incommensurate), but that we have also displacements between different sites. This is the key signal for superfluidity. We also show in the same figure the $x - y$ static structure factors for both phases. As expected, the one for the glass does not show any Bragg peak and looks rather similar to $S(k)$ for a liquid at the same density. Instead, the triangular crystal shows a clear Bragg peak, but relatively small due to the delocalization of particles.

In this work, we have studied the adsorption of H_2 on an amorphous substrate. To do so, we have used a set of coordinates that were supposed to model adequately an amorphous two-dimensional carbon material experimentally obtained [10]. We considered a both a flat substrate and a corrugated one. Surprisingly, the results are quite similar in one important question: there is at least a region around 0.055 \AA^{-2} for which we have an stable glass. We have also found that the superfluid density of that glass can be tiny or sizable, but not zero. This result is compatible with a recent calculation for the second layer of H_2 on graphite [14] that found a tiny supersolid density in a very thin density region. As in that work, we can ascribe the superfluidity to the relative low density of the glass at equilibrium. This prompts us to suggest that we can expect to find a superglass in a real disordered substrate similar to that of Ref. 10. In the worst case scenario, a superfluid density of the order of the one we found for the flat substrate can be detected using the perfected torsional oscillator technique used in Ref. 21 for ^4He on graphite.

ACKNOWLEDGMENTS

We acknowledge financial support from Ministerio de Ciencia e Innovación MCIN/AEI/10.13039/501100011033 (Spain) under Grants No. PID2020-113565GB-C22 and No. PID2020-113565GB-C21, and from Junta de Andalucía group PAIDI-205. M.C.G. acknowledges funding from Fondo Europeo de Desarrollo Regional (FEDER) and Consejería de Economía, Conocimiento, Empresas y Universidad de la Junta de Andalucía, en marco del programa operativo FEDER Andalucía 2014-2020. Objetivo específico 1.2.3. “Fomento y generación de conocimiento frontera y de conocimiento orientado a los retos de la sociedad, desarrollo de tecnologías emergentes” under Grant No. UPO-1380159. Porcentaje de cofinanciación FEDER 80%. J.B. acknowledges financial support from Secretaria d’Universitats i Recerca del Departament d’Empresa i Coneixement de la Generalitat de Catalunya, cofunded by the European Union Regional Development Fund within the ERDF Operational

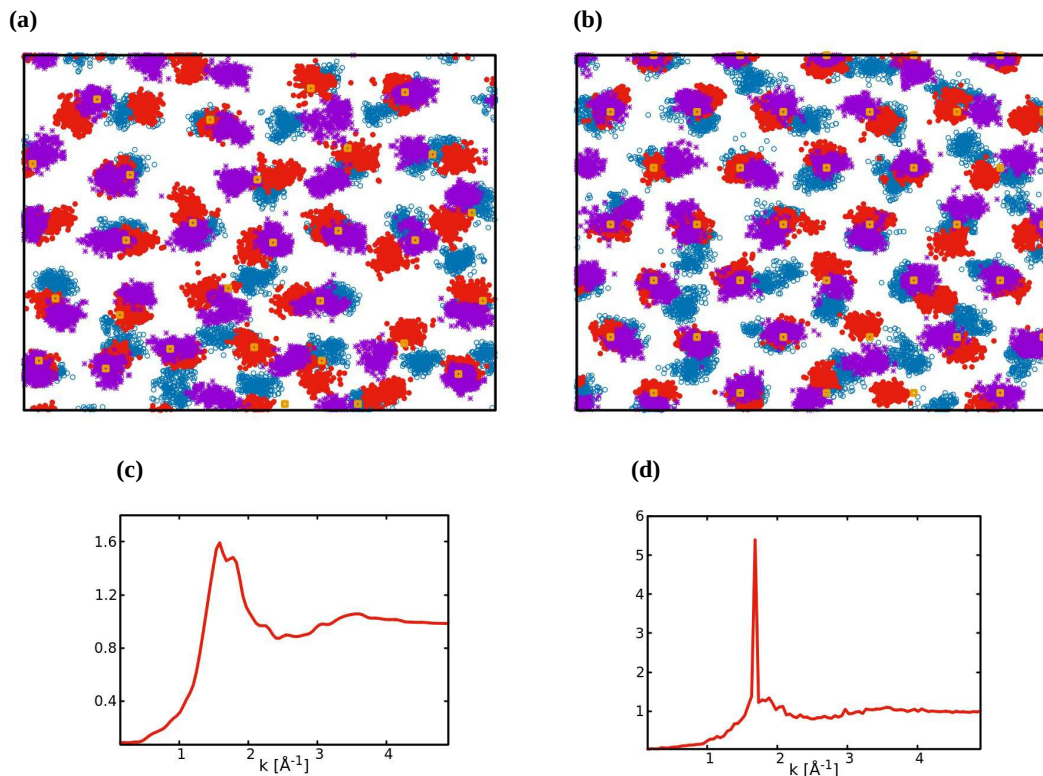


FIG. 5. **(a)** Snapshots representing different sets of $x-y$ configurations corresponding to different Monte Carlo steps for a glass phase of density 0.055 \AA^{-2} . Different colors stand for different simulation steps. The yellow squares represent the positions of the nodes of the glass network. **(b)** Same for an incommensurate solid of density 0.065 \AA^{-2} . Now the squares correspond to the crystallographic positions of a triangular lattice. **(c)-(d)**: Static structure factors for the glass and incommensurate crystal, respectively.

Program of Catalunya (project QuantumCat, Ref. No. 001-P-001644). We also acknowledge the use of the

C3UPO computer facilities at the Universidad Pablo de Olavide.

-
- [1] K. S. Novoselov, A. K. Geim, S. V. Morozov, D. Jiang, Y. Zhang, S. V. Dobonos, I. V. Grigorieva, and A. A. Firsov, Electric field effect in atomically thin carbon films, *Science* **306**, 666 (2004).
- [2] K. S. Novoselov, D. Jiang, F. Schedin, T. J. Booth, V. V. Khotkevich, S. V. Morozov, and A. K. Geim, Two-dimensional atomic crystals, *Proc. Natl. Acad. Sci. U.S.A.* **102**, 10451 (2005).
- [3] K. S. Novoselov, A. K. Geim, S. V. Morozov, D. Jiang, M. I. Katsnelson, I. V. Grigorieva, S. V. Dubonos, and A. A. Firsov, Two-dimensional gas of massless dirac fermions in graphene, *Nature (London)* **438**, 197 (2005).
- [4] Y. Zhang, Y. Tan, H. L. Stormer, and P. Kim, Experimental observation of the quantum hall effect and berry's phase in graphene, *Nature (London)* **438**, 201 (2005).
- [5] M. C. Gordillo and J. Boronat, ^4He on a single graphene sheet, *Phys. Rev. Lett.* **102**, 085303 (2009).
- [6] M. C. Gordillo and J. Boronat, Phase diagram of H_2 adsorbed on graphene, *Phys. Rev. B* **81**, 155435 (2010).
- [7] C. Carbonell-Coronado and M. C. Gordillo, Phase diagram of D_2 adsorbed on graphene and graphite, *Phys. Rev. B* **85**, 155427 (2012).
- [8] J. Kotakoski, A. V. Krasheninnikov, U. Kaiser, and J. C. Meyer, From point defect in graphene to two-dimensional amorphous carbon, *Phys. Rev. Lett.* **106**, 105505 (2011).
- [9] F. R. Eder, J. Kotakoski, U. Kaiser, and J. C. Meyer, A journey from order to disorder. Atom by atom transformation from graphene to a 2D carbon glass, *Sci. Rep.* **4**,

- 4060 (2014).
- [10] C. Toh, H. Zhang, J. Lin, A. S. Mayorov, Y. Wang, C. M. Orofeo, D. B. Ferry, H. Andersen, N. Kakenov, Z. Guo, I. H. Abidi, H. Sims, K. Suenaga, S. T. Pantelides, and B. Ozyilmaz, Synthesis and properties of free-standing monolayer amorphous carbon, *Nature (London)* **577**, 199 (2020).
- [11] O. N. Osychenko, R. Rota, and J. Boronat, Superfluidity of metastable glassy bulk para-hydrogen at low temperature, *Phys. Rev. B* **85**, 224513 (2012).
- [12] J. Boronat, in *Microscopic Approaches to Quantum Liquids in Confined Geometries*, edited by E. Krotscheck and J. Navarro (World Scientific, Singapore, 2002).
- [13] M. C. Gordillo and J. Boronat, Second layer of H₂ and D₂ adsorbed on graphene, *Phys. Rev. B* **87**, 165403 (2013).
- [14] M. C. Gordillo and J. Boronat, Supersolidity in the second layer of para-H₂ adsorbed on graphite, *Phys. Rev. B* **105**, 094501 (2022).
- [15] G. Stan and M. W. Cole, Hydrogen adsorption in nanotubes, *J. Low Temp. Phys.* **110**, 539 (1998).
- [16] I. F. Silvera and V. V. Goldman, The isotropic intermolecular potential for H₂ and D₂ in the solid and gas phases, *J. Chem. Phys.* **69**, 4209 (1978).
- [17] Y. Li, F. Inam, A. Kumar, M. F. Thorpe, and D. A. Drabold, Pentagonal puckering in a sheet of amorphous graphene, *Phys. Status Solidi (b)* **248**, 2082 (2011).
- [18] R. Thapa, C. Ugwumadu, K. Nepal, J. Trembly, and D. A. Drabold, Ab initio simulation of amorphous graphite, *Phys. Rev. Lett.* **128**, 236402 (2022).
- [19] M. C. Gordillo and J. Boronat, *Phys. Rev. Lett.* **124**, 205301 (2020).
- [20] S. Zhang, and N. Kawashima, J. Carlson, and J. E. Gubernatis, Quantum simulations of the superfluid-insulator transition for two-dimensional, disordered, hard-core bosons, *Phys. Rev. Lett.* **74**, 1500 (1995).
- [21] J. Choi, A.A. Zadorozhko, Jeakyung. Choi, and E. Kim, Spatially modulated Superfluid State in two-dimensional ⁴He films, *Phys. Rev. Lett.* **127**, 135301 (2021).